Journal of Applied Polymer Science

Fabrication of mPEGylated graphene oxide/poly(2-dimethyl aminoethyl methacrylate) nanohybrids and their primary application for small interfering RNA delivery

Yu Sun,[1†] Junhui Zhou,[1†] Qiang Cheng,[2] Daoshu Lin,[1] Qian Jiang,[2] Anjie Dong,[1,3,4] Zicai Liang,[2] Liandong Deng[1]

[1]Department of Polymer Science and Technology, School of Chemical Engineering and Technology, Tianjin University, Tianjin 300072, People's Republic of China

[2]Laboratory of Nucleic Acid Technology, Institute of Molecular Medicine, Peking University, Beijing 100871, People's Republic of China

[3]Key Laboratory of Systems Bioengineering (Ministry of Education), Tianjin 300072, People's Republic of China

[4]Collaborative Innovation Center of Chemical Science and Engineering (Tianjin), Tianjin 300072, People's Republic of China

Yu Sun and Junhui Zhou contributed equally to this work.

Correspondence to: Z. Liang (E-mail: liangz@pku.edu.cn) and L. Deng (E-mail: dengliandong@aliyun.com)

ABSTRACT: Graphene oxide (GO)-based nanohybrids were designed for small interfering RNA (siRNA) delivery for their high water dispensability, good biocompatibility, easily tunable surface functionalization, and particular optical properties. In this study, novel nanohybrids based on GO were fabricated. Methoxypoly(ethylene glycol) (mPEG) was covalently conjugated to GO via amide bonds. Then, poly(2-dimethyl aminoethyl methacrylate) (PDMAEMA), which was synthesized via reversible addition–fragmentation chain transfer polymerization (RAFT) with 2-(dodecyl thiocarbonothioyl thio)-2-methyl propionic acid (DTM) as the RAFT agent, was attached onto GO via physical interaction between DTM and GO. Compared with Lipofectamine 2000, the novel mPEG–GO/PDMAEMA nanohybrids showed comparable gene transfection efficiency and a low cytotoxicity. Moreover, the mPEG–GO/PDMAEMA nanohybrids showed enhanced optical properties compared to the original GO because of the presence of mPEG and PDMAEMA. Our work encouraged further exploration of the novel nanovector for combined photothermal and siRNA delivery. © 2015 Wiley Periodicals, Inc. J. Appl. Polym. Sci. **2016**, *133*, 43303.

KEYWORDS: biocompatibility; biomaterials; composites; graphene and fullerenes; nanotubes

Received 29 August 2015; accepted 27 November 2015

DOI: 10.1002/app.43303

INTRODUCTION

Small interfering RNA (siRNA) is a promising therapeutic platform for modulating gene-related diseases, and it has been investigated in the past decade since its debut.[1–3] Nowadays, siRNA has emerged as the most innovative nucleic acid medicine.[4,5] However, there exist significant challenges in the systemic delivery of siRNA. The delivery of appropriate siRNA into targeted cells is a key step in gene therapy.[6] Therefore, so far, tremendous efforts have been devoted to seeking efficient and safe gene carriers; these include liposomes,[7,8] polycations,[9–11] nanomaterials (e.g., silica nanoparticles, gold nanoparticles, calcium phosphate nanoparticles).[12–15]

Recently, graphene oxide (GO), a precursor of graphene, has been proven to be one kind of promising material. GO holds multiple distinct advantages over other nonviral vectors;[16] these include a high water dispensability, facile synthesis, easily tunable surface functionalization, and good biocompatibility.[17–19] Functionalized GO has potential applications in drug delivery,[20] cellular imaging,[21,22] and photothermal therapy.[23,24] At present, numerous research groups have done a lot of work, and thus, a variety of GO-based platforms have been developed. For example, Huang and coworkers[26,27] reported the covalent modification of graphene with polymers by azide/alkyne click chemistry,[25] atom-transfer nitroxide radical coupling chemistry, or single-electron-transfer nitroxide radical coupling chemistry. The most popular method is chemical modification through 1-ethyl-3-[3-(dimethyl amino)propyl] carbodiimide hydrochloride (EDC) chemistry. Dai *et al.*[28] demonstrated for the first time that poly(ethylene glycol)

†Yu Sun and Junhui Zhou contributed equally to this work.

(PEG) could render a high aqueous solubility and stability of GO in physiological solutions. Liu and coworkers[29,30] also demonstrated that the presence of PEG enhanced the optical properties of GO.[24] The PEGylation of graphene could make it a desired carrier for the delivery of hydrophobic anticancer drugs. As for gene therapy, polyethylenimine-functionalized GO was fabricated as an efficient gene-delivery vector.[31,32] To further improve the solubility and stability of GO-based gene carriers, PEG–polyethylenimine–GO as a new platform was synthesized through covalent chemical conjugation.[22,33] In addition to chemical modification, various GO-based derivatives were fabricated through noncovalent physisorption. For example, Liu *et al.*[34] fabricated a pyrene-terminated poly(2-dimethyl aminoethyl methacrylate) (PDMAEMA)–PEG and attached it to the graphene surface via π–π stacking interactions. However, even though tremendous progress has been achieved, few nanovectors combine photothermal properties and siRNA delivery. Our work highlighted the fact that GO with appropriate surface modification is promising for gene delivery and that methoxypoly (ethylene glycol) (mPEG) and PDMAEMA can be used to enhance the optical properties of GO for photothermal therapy in future research. In addition, the method of fabrication was simplified.

In this study, novel mPEG–GO/PDMAEMA nanohybrids for gene delivery were prepared. To simplify the fabrication process, both chemical modification and noncovalent physisorption were combined. During the synthesis of mPEG–GO, EDC chemistry was used first. Then, PDMAEMA was synthesized through the adoption of 2-(dodecyl thiocarbonothioyl thio)-2-methyl propionic acid (DTM) as a RAFT agent; this was then attached to the surface of mPEG–GO through the interaction between DTM and GO.[35–37] Moreover, the influences of the presence of mPEG and PDMAEMA on the optical properties of GO were investigated with ultraviolet–visible–near-infrared (UV–vis–NIR) spectroscopy. In addition, the cytotoxicity of the mPEG–GO/PDMAEMA/siRNA complexes to HeLa–Luc cells was evaluated with the MTT method in which 3-(4,5-dimethylthiazol-2-yl)-2,5-diphenyl tetrazolium bromide (MTT) was applied to assess cell viability. Furthermore, siRNA's knockdown efficiency *in vitro* was examined.

EXPERIMENTAL

Materials

GO powder was purchased from Alfa Aesar. EDC and *N*-hydroxysuccinimide (NHS) were obtained from Aladdin. 2-Dimethyl aminoethyl methacrylate (DMAEMA) and α,α-azoisobutyronitrile (AIBN) was purchased from Alfa Aesar. Methoxypoly(ethylene glycol) amine HCl salt (mPEG–NH_2 HCl) was purchased from Jenkem Technology.

Synthesis of mPEG–GO

Before the conjugation of mPEG to GO, the purchased GO was dispersed in deionized water through sonication for 1 h. As shown in Scheme 1(a), EDC and NHS were added to the GO dispersion in a vial to activate the carboxyl groups of GO. Subsequently, mPEG–NH_2 HCl was added to the activated GO solution. Then, the mixture was stirred at room temperature for 1 day. Finally, excess mPEG, EDC, and NHS were removed by a dialysis method through a membrane with a 3.5-kDa molecular weight cutoff to obtain mPEG–GO.

Synthesis and Characterization of DTM–PDMAEMA

DTM was synthesized according to a previously described procedure[38] in our laboratory. DTM–PDMAEMA was synthesized by RAFT with DTM as the RAFT agent, as shown in Scheme 1(b). Typically, DTM (72.92 mg, 0.2 mmol), DMAEMA (1257.68 mg, 8 mmol), AIBN (3.28 mg, 0.02 mmol), and tetrahydrofuran (THF; 3 mL) were added to a 25-mL Schlenk tube at one time. The mixture was degassed through three freeze–pump–thaw cycles. The Schlenk tube was placed in an oil bath at 70°C for about 24 h under an argon atmosphere; the tube was immersed in liquid nitrogen to quench the polymerization. After that, the polymer solution was dialyzed against water with a membrane with a 3.5-kDa molecular weight cutoff and then lyophilized. The chemical stricture and molecular weight of PDMAEMA were measured with an ^{1}H-NMR instrument (Varian Unity-Plus INOVA 500) and gel permeation chromatography (GPC) instrument equipped with a PLgel Organic GPC column (10-μm Mixed-B, Org 300 $\times$ 7.8 mm^2) with an RI2000 detector.

Preparation and Characterization of the mPEG–GO/PDMAEMA Nanohybrids

Herein, the PDMAEMA was coated on the surface of mPEG–GO through noncovalently interaction, as shown in Scheme 1(c). In the preparation of the mPEG–GO/PDMAEMA nanohybrids, the mPEG–GO was dispersed in PDMAEMA solutions by sonication for 60 min; this yielded a black suspension, which was centrifuged at 8000 rpm to remove unstable aggregates. After repeated water washing, the mPEG–GO/PDMAEMA nanohybrids collected on filter membranes were resuspended in water through brief sonication and centrifuged at 8000 rpm for 10 min to remove any aggregates formed during the filtration step. The mPEG–GO/PDMAEMA nanohybrids were stored as the suspension, and part of the mPEG–GO/PDMAEMA nanohybrids were freeze-dried for further characterization. The chemical structure of the mPEG–GO/PDMAEMA nanohybrids was confirmed by Fourier transform infrared spectroscopy (Bruker Vector-22 IR spectrometer) with a KBr pellet. The successful loading of PDMAEMA to mPEG–GO was then measured by UV–vis–NIR spectroscopy, and the relative amount of mPEG and PDMAEMA in the mPEG–GO/PDMAEMA nanohybrids was confirmed by X-ray photoelectron spectroscopy (XPS; PerkinElmer Phi 1600 electron spectroscopy for chemical analysis system) with Mg Kα (1254.0 eV) as the radiation source.

The surface morphologies of the GO, mPEG–GO, and mPEG–GO/PDMAEMA nanohybrids were determined by scanning electron microscopy (SEM; an Hitachi H-7650 instrument operating at an acceleration voltage of 3.0 kV). GO, mPEG–GO, and mPEG–GO/PDMAEMA nanohybrids dispersions (~0.1 mg/mL) with one droplet, respectively, were dropped into freshly prepared silicon wafers, which were then dried at room temperature. Finally, the samples were observed by SEM after a gold-sputtering treatment.

ζ Potential Measurements

The surface charges of the GO, mPEG–GO, and mPEG–GO/PDMAEMA nanohybrids in PBS buffer (pH 7.4) were confirmed by ζ potential measurements with a Nano Z Zetasizer (Malvern Instruments, Malvern, United Kingdom).

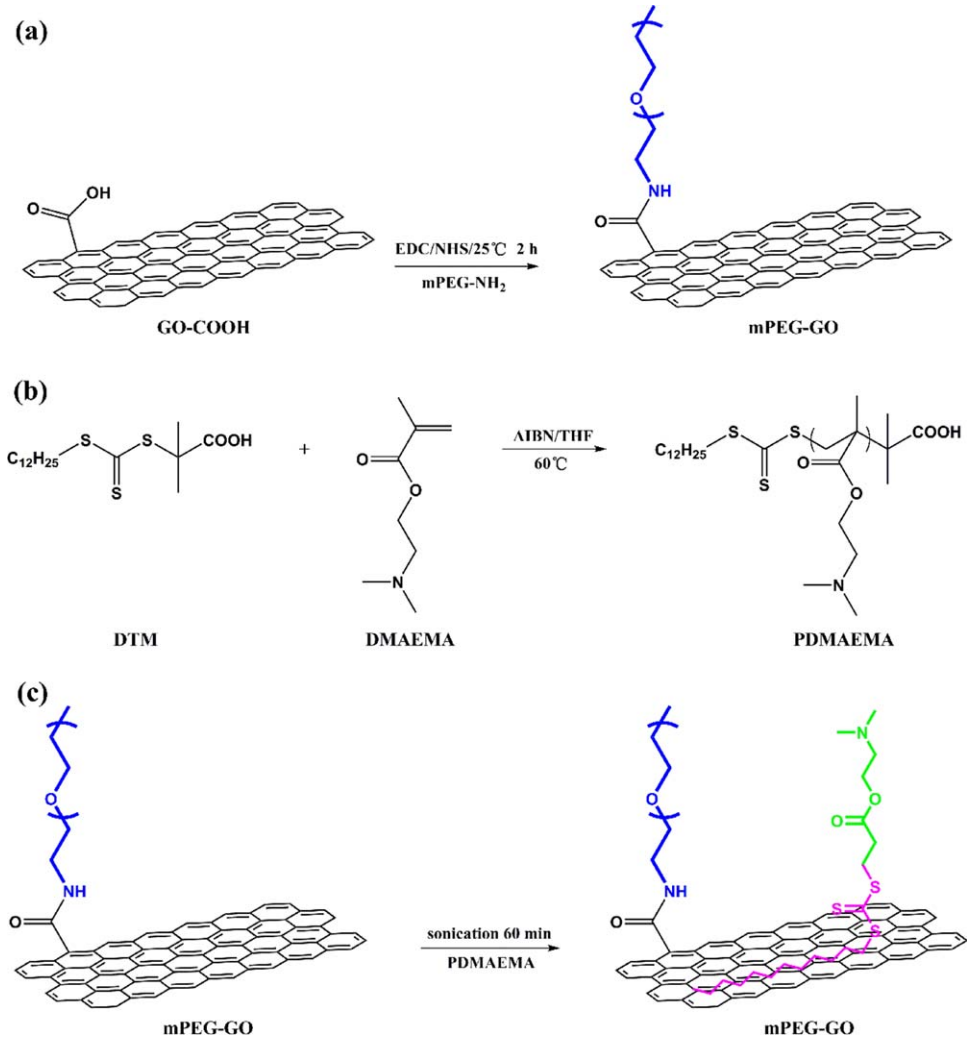

Scheme 1. (a) Synthesis of the mPEG–GO conjugate, (b) preparation of PDMAEMA via RAFT, and (c) preparation of the mPEG–GO/PDMAEMA complexes. [Color figure can be viewed in the online issue, which is available at wileyonlinelibrary.com.]

Agarose Gel Retardation Assay

mPEG–GO/PDMAEMA/siRNA complexes were prepared through the addition of mPEG–GO/PDMAEMA nanohybrids suspension to the siRNA solution at various N/P ratios from 0 to 30 in diethylpyrocarbonate (DEPC) and then incubated for 1 h at room temperature. The mPEG–GO/PDMAEMA/siRNA complexes were mixed with 4 μL of 6× loading buffer (Takara Biotechnology, Dalian, Liaoning Province, China), and then, the mixture was added to a 2% agarose gel containing 5 μg/mL ethidium bromide. Electrophoresis was carried out at a voltage of 120 V for 20 min in 1× Tris-acetate-EDTA (TAE) running buffer. Finally, the results were recorded at a UV light wavelength of 254 nm with an Image Master video data sequences (VDS) thermal imaging system (Bio-Rad, Hercules, CA).

Cell Viability Assays

The *in vitro* cytotoxicity of the mPEG–GO/PDMAEMA/siRNA complexes was investigated by MTT assay. HeLa–Luc, a luciferase-steady expressional cell line, was used to evaluate the MTT assay. First, HeLa–Luc cells were seeded in 96-well plates (1×10^4 cells/well), which were treated with the complexes containing 0.25 μg of siRNA and then incubated for 24 h. Later, 5 μL of MTT solution was added to each well. After incubation for 4 h, 50 μL of dimethyl sulfoxide was added to each well and further incubated for 30 min at 37°C. The absorbance of the solution was measured at 570 nm with a microplate reader. The results were expressed as a percentage of the absorbance of the blank control.

In Vitro Luciferase Gene Silencing

To verify the cellular transfection of the mPEG–GO/PDMAEMA/siRNA complexes, gene knockdown was evaluated in a modified HeLa cell line where the HeLa cells were genetically engineered to express luciferase. In the gene knockdown study, luciferase activity was adopted as an indicator of the magnitude of the silencing effect. Lipofectamine 2000 was used as the positive control. Before the gene silencing experiments, the HeLa–Luc cells were plated in 24-well culture plates at an initial density of 5×10^4 cells per well and incubated for 1 day before transfection. As before, the transfection experiment was performed with three

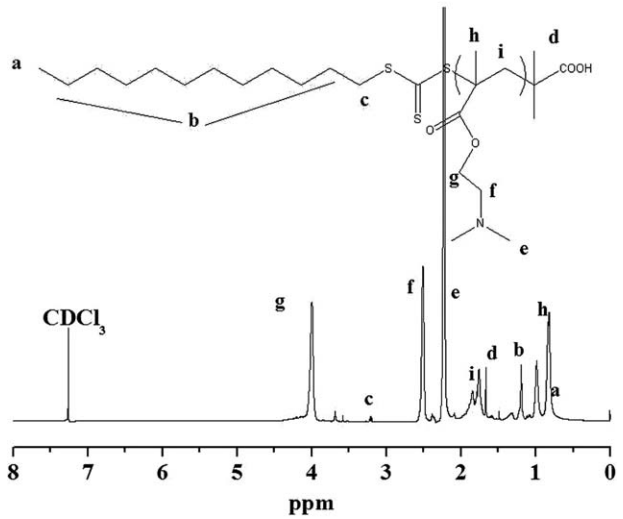

Figure 1. ^{1}H-NMR spectrum of PDMAEMA in $CDCl_3$.

wells per sample. After 24 h of incubation, the medium was removed, and the cells were washed twice with PBS. Then, the cells were lysed with 200 mL of 1× reporter lysis buffer (Promega Co., Madison, WI); this was followed by violent shaking for 30 min to ensure complete lysis. The cell lysate was transferred into a 1.5-mL centrifuge vial and centrifuged for 30 s at 12,000 rpm. Then, the supernatant was collected for luminescence measurements. The fluorescence intensity was measured with a fluorometer (Synergy HT, BioTek).

RESULTS AND DISCUSSION

Synthesis and Characterization of PDMAEMA

To develop the GO-based gene-delivery carrier, PDMAEMA [weight-average molecular weight (M_w) = 5.5 kDa] was synthesized via RAFT with DTM as the RAFT agent [Scheme 1(b)]. The chemical composition and molecular weight of PDMAEMA were determined by ^{1}H-NMR and GPC. As shown in Figure 1, the characteristic peaks of PDMAEMA were exhibited. Sharp peaks at 0.83 ppm (terminal CH_3, a), 1.25 ppm (CH_2CH_2, b), 3.21 ppm [C(=S)—S—CH_2, c], and 1.65 ppm (CH_3, d) were attributed to the methyl and methylene protons of the DTM, and the characteristic peaks of PDMAEMA were observed at δ values of about 0.97 (h), 1.75 (i), 4.00 (g), 2.50 (f), and 2.20 (e) ppm. These results confirmed the formation of PDMAEMA.

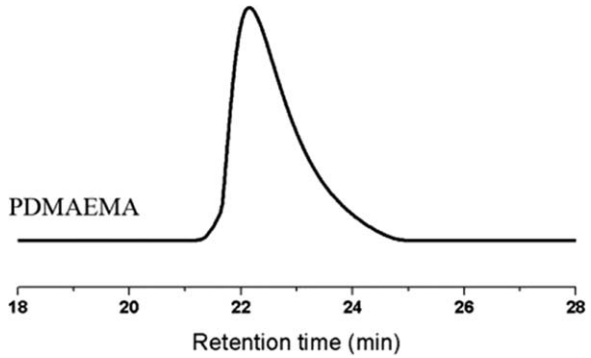

Figure 2. GPC elution chromatogram of PDMAEMA.

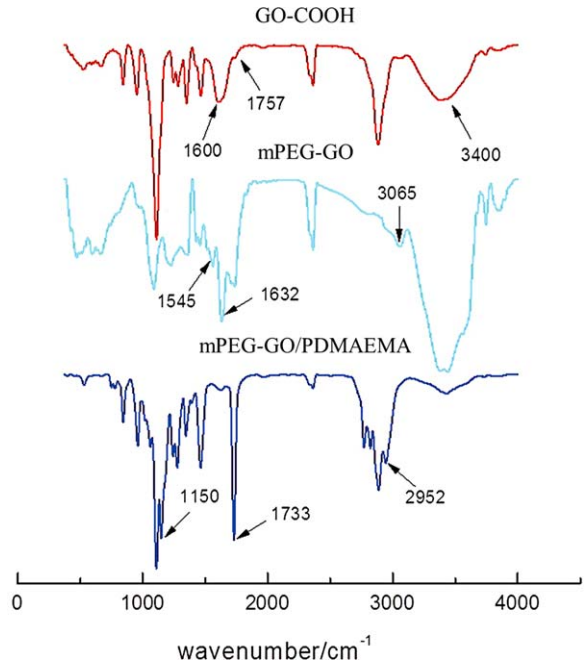

Figure 3. IR spectra of GO–COOH, mPEG–GO, and mPEG–GO/PDMAEMA. [Color figure can be viewed in the online issue, which is available at wileyonlinelibrary.com.]

The peak intensities of the hydrogen protons on the methyl of DMAEMA ($\delta \approx 2.20$, e) and methylene protons of DTM ($\delta \approx 1.25$, b) were used to calculate the chemical composition and number-average molecular weight (M_n) of PDMAEMA. The GPC curve of PDMAEMA with a narrow molecular weight distribution ($M_w/M_n = 1.10$) is shown in Figure 2. We found that the molecular weight calculated from ^{1}H-NMR ($M_n = 4.9$ kDa) and the molecular weight determined by GPC ($M_n = 5.1$ kDa) were both in good agreement with the theoretical values; this indicated the well-controlled nature of RAFT.

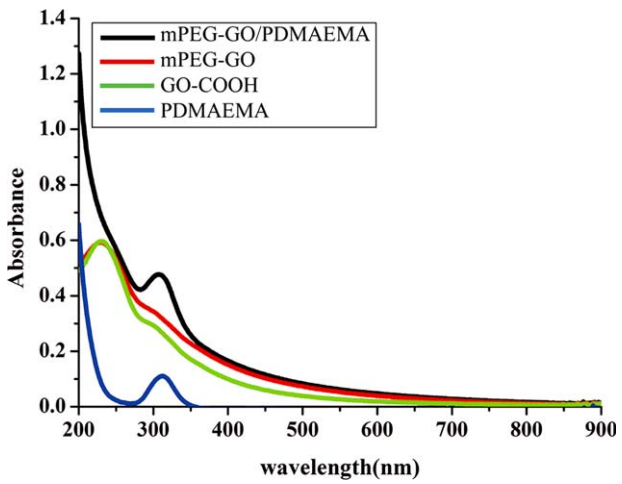

Figure 4. UV–vis–NIR spectra of GO–COOH, mPEG–GO, and mPEG–GO/PDMAEMA at a GO concentration of 0.1 mg/mL and PDMAEMA at a concentration of 0.1 mg/mL. [Color figure can be viewed in the online issue, which is available at wileyonlinelibrary.com.]

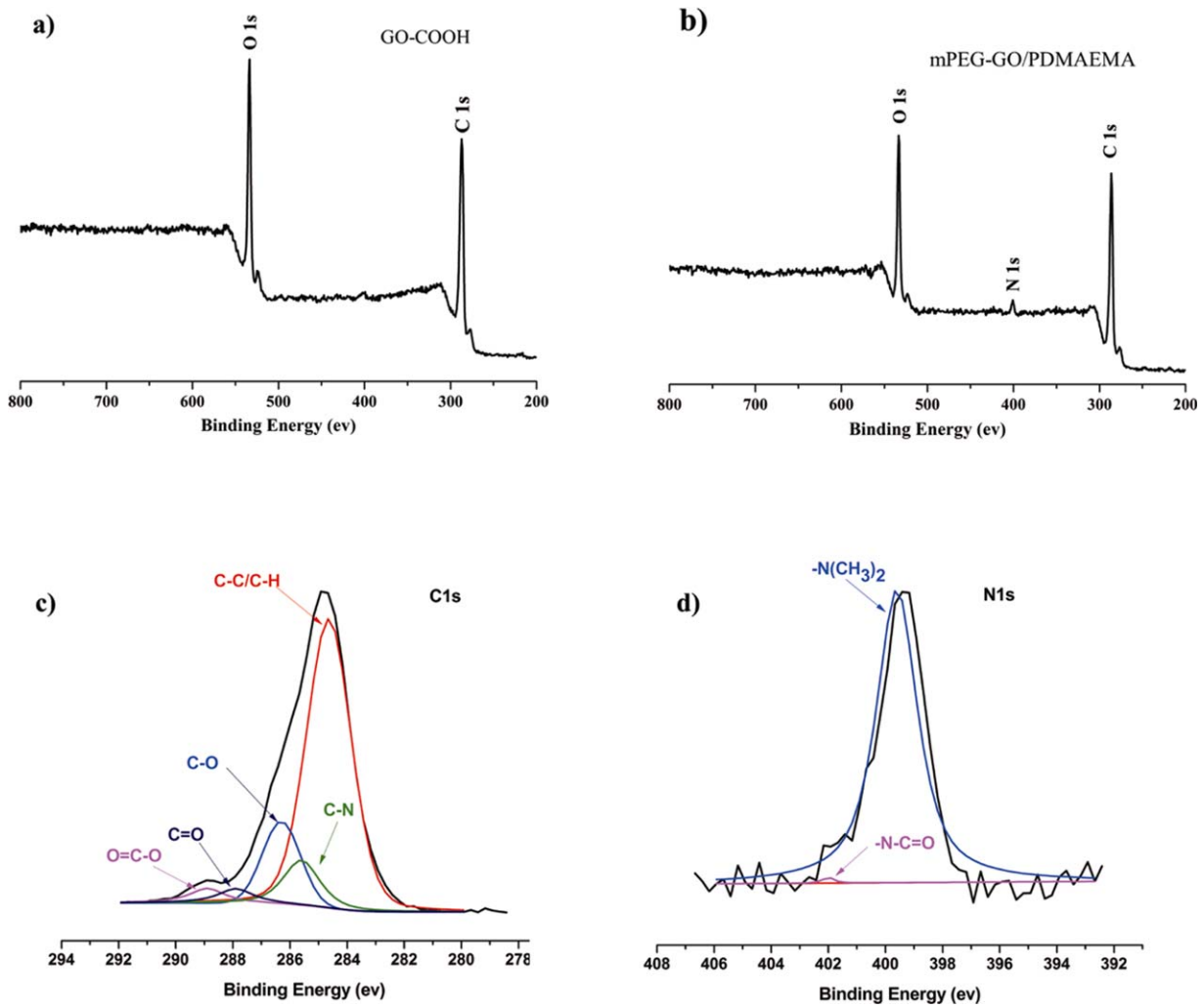

Figure 5. XPS spectra: (a) survey spectra of GO–COOH, (b) survey spectra of mPEG–GO/PDMAEMA, (c) C1s narrow scan of mPEG–GO/PDMAEMA, and (d) N1s narrow scan of mPEG–GO/PDMAEMA. [Color figure can be viewed in the online issue, which is available at wileyonlinelibrary.com.]

Characterization of the mPEG–GO/PDMAEMA Nanohybrids

To improve the biocompatibility of the GO-based gene-delivery carriers, mPEG–NH_2 (M_w = 5.0 kDa) was covalently conjugated to the carboxyl group of GO with EDC/NHS chemistry [Scheme 1(a)]. Then, mPEG–GO/PDMAEMA nanohybrids were prepared according to the described steps. After freeze drying, the resulting nanohybrids were characterized by Fourier transform infrared spectroscopy, UV–vis–NIR spectroscopy, XPS, and SEM, as shown in Figures 3–6, respectively. As shown in Figure 3, IR spectroscopy revealed the existence of OH (~3400 cm^{-1}), COOH (1757 cm^{-1}), and C═C─C═C (1600 cm^{-1}) functional groups in the GO–COOH. After the conjugation of the amino of mPEG and the carboxyl group of GO, the IR characterization of carefully purified mPEG–GO samples indicated NH (3065 cm^{-1}) vibrations, C═O (1545 cm^{-1}), and characteristic amide–carbonyl (NH─CO) stretching vibrations (~1632 cm^{-1}); this was consistent with the grafting of the mPEG molecules onto GO sheets. After mPEG–GO was mixed with PDMAEMA, IR characterization of the carefully purified mPEG–GO/PDMAEMA samples indicated CH_3 (2952 cm^{-1}) vibrations, C═O (1733 cm^{-1}), and C(O)─O (1150 cm^{-1}); this suggested the successful fabrication of the mPEG–GO/PDMAEMA nanohybrids.

Additional evidence that the mPEG–GO/PDMAEMA nanohybrids were successfully formed was provided by UV–vis–NIR spectroscopy. As shown in Figure 4, the UV–vis–NIR spectrum of the nanohybrids revealed mPEG–GO peaks superimposed with the absorption curve of PDMAEMA; this suggested the successful preparation of the mPEG–GO/PDMAEMA nanohybrids.

The XPS spectrum of GO–COOH is shown in Figure 5(a). It provided evidence for the presence of three elemental species C, N, and O in Figure 5(b). The mPEG–GO/PDMAEMA nanohybrids contained 33.7% PDMAEMA by theoretical calculations, according to the spectral intensities observed in the experiments. Figure 5(c,d) present the C1s and N1s narrow scans, respectively. As shown in Figure 5(c), the C1s narrow scan consisted of five components, among which the component centered at 286.2 eV was assigned to the C─O─C of mPEG. As shown in Figure 5(d), the N1s narrow scan had two peaks at 398.5 and 402.1 eV; these were assigned to ─$N(CH_3)_2$ of PDMAEMA and ─N─C═O of mPEG–GO, respectively.

The morphologies of the GO, mPEG–GO, and mPEG–GO/PDMAEMA nanohybrids were investigated by SEM. As shown

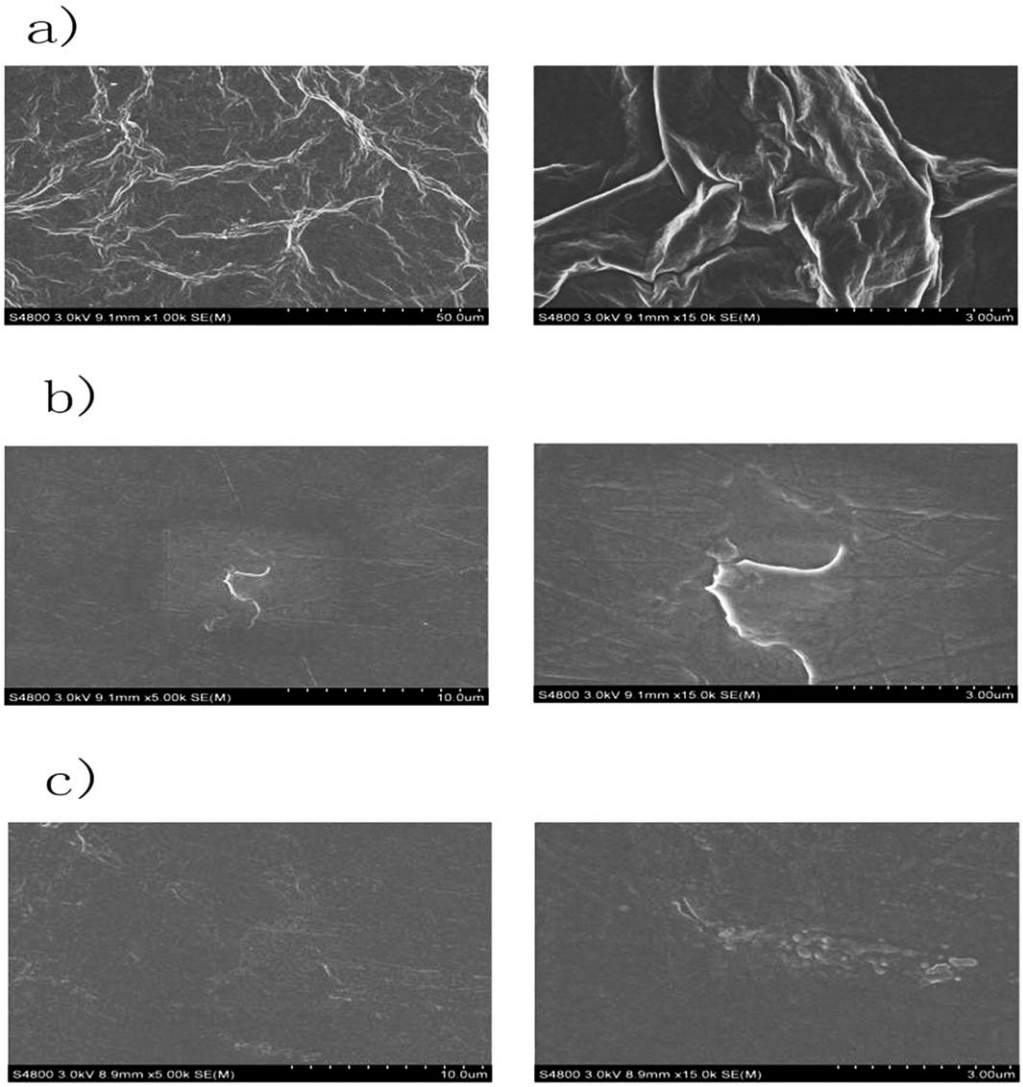

Figure 6. SEM of (a) GO–COOH, (b) mPEG–GO, and (c) mPEG–GO/PDMAEMA.

in Figure 6(a), a lot of folds on the surface of the original GO–COOH were observed. As shown in Figure 6(b), a majority of folds on the surface disappeared after the conjugation of mPEG with GO; this may have been because of the mPEG on the surface of GO. As shown in Figure 6(c), those folds were seldom seen with PDMAEMA absorption on the surface of mPEG–GO; this may have been due to the increased amount of polymer on the surface.

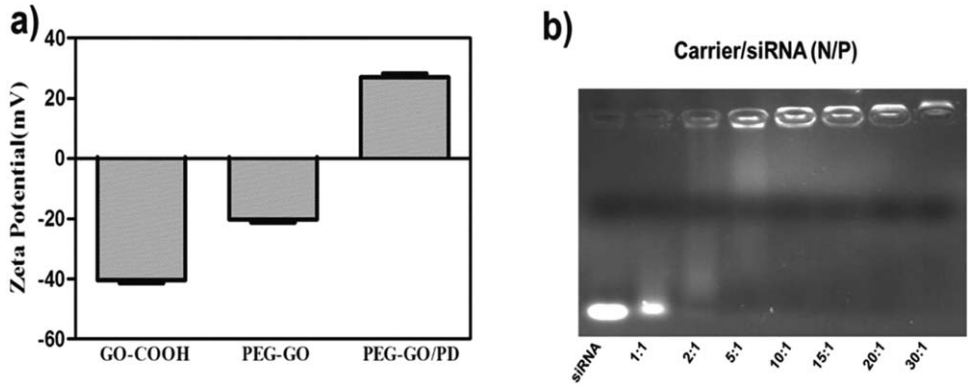

Figure 7. (a) ζ potential of GO–COOH, mPEG–GO, and mPEG–GO/PDMAEMA at a concentration of 0.1 mg/mL and (b) agarose gel retardation study of siRNA complexed with mPEG–GO/PDMAEMA at various N/P ratios.

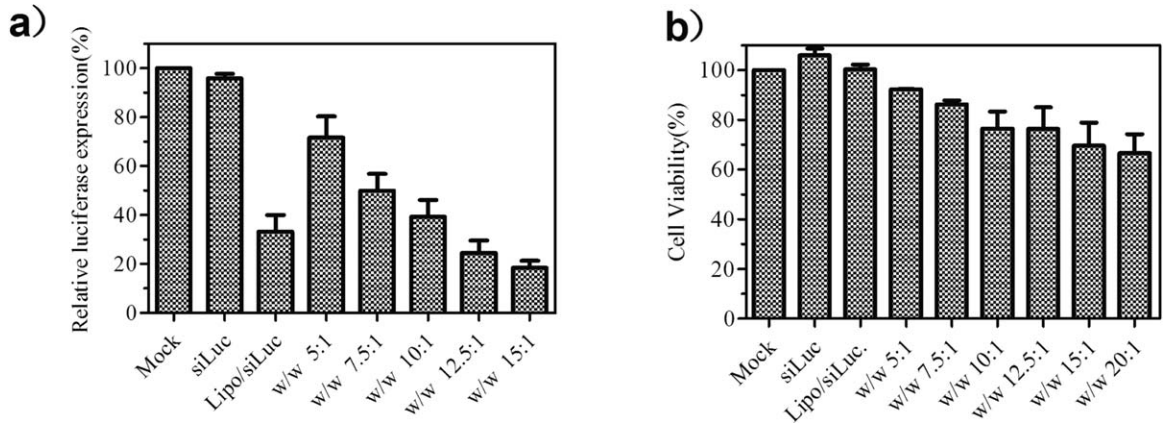

Figure 8. (a) Luciferase expression silencing in the HeLa–Luc cells and (b) cytotoxicity of the mPEG–GO/PDMAEMA/siRNA complexes to the HeLa–Luc cells.

Complexation of mPEG–GO/PDMAEMA with siRNA

The ζ potentials of the mPEG, mPEG–GO, and mPEG–GO/PDMAEMA nanohybrids were investigated by ζ potential measurements. As shown in Figure 7(a), the ζ potential of GO–COOH was about −40 mV, whereas the ζ potential of mPEG–GO was about −20 mV because mPEG was conjugated with GO. After the absorption of PDMAEMA, the ζ potential of the mPEG–GO/PDMAEMA nanohybrids turned from negative to positive and reached 29 mV because of the immobilized cationic polymer PDMAEMA, which was critical to successful complexation with siRNA. The loading capability of the mPEG–GO/PDMAEMA nanohybrids as a gene carrier was investigated by agarose gel assay. As shown in Figure 7(b), the complete retardation of siRNA was achieved when the weight ratio of the mPEG–GO/PDMAEMA nanohybrids to siRNA was higher than 10; this suggested the complete condensation of siRNA.

Gene Silencing Efficiency of the mPEG–GO/PDMAEMA/siRNA Complexes

To investigate the potential of the mPEG–GO/PDMAEMA nanohybrids as an efficient gene carrier, the siRNA transfection activities of the mPEG–GO/PDMAEMA/siRNA complexes were examined with HeLa–Luc cells. As shown in Figure 8(a), compared to naked siRNA, the mPEG–GO/PDMAEMA/siRNA complexes enhanced the luciferase silencing efficiency remarkably. The level of luciferase expression was reduced gradually by the transfection of the mPEG–GO/PDMAEMA/siRNA complexes with the increasing weight ratio of the mPEG–GO/PDMAEMA nanohybrids to siRNA. Moreover, the mPEG–GO/PDMAEMA/siRNA complexes reached gene knockdown efficiencies comparable to those of Lipofectamine 2000/siRNA (Lipo/siLuc) when the weight ratio of the mPEG–GO/PDMAEMA nanohybrids to siRNA reached 12.5. Hence, the mPEG–GO/PDMAEMA nanohybrids enhanced the gene silencing efficiency of siRNA more efficiently.

Table I. UV–vis–NIR Spectra of GO–COOH, mPEG–GO, and mPEG–GO/PDMAEMA at 808 nm at a Concentration of 0.1 mg/mL

	Absorbance
GO-COOH	0.0070
mPEG-GO	0.0119
mPEG-GO/PDMAEMA	0.0159

In Vitro Cytotoxicity of the mPEG–GO/PDMAEMA/siRNA Complexes

The cytotoxicity of a gene vector is critical for its practical applications in gene therapy. The toxicity of the mPEG–GO/PDMAEMA/siRNA complexes was evaluated by the MTT assay with HeLa–Luc cells. As shown in Figure 8(b), the cell viability decreased when the weight ratio of the mPEG–GO/PDMAEMA nanohybrids to siRNA increased; this was mainly because of the strong positive charge inducing intense interactions with cell membranes. Although the toxicity of the mPEG–GO/PDMAEMA nanohybrids to HeLa cells increased when the weight ratio of the mPEG–GO/PDMAEMA nanohybrids to siRNA increased, the viable cells reached 80% when the weight ratio of mPEG–GO/PDMAEMA nanohybrids to siRNA was 12.5. Coupled with the results of the gene silencing efficiency study, we drew the conclusion that the mPEG–GO/PDMAEMA nanohybrids could deliver siRNA more efficiently with a relatively low toxicity.

Optical Properties of the mPEG–GO/PDMAEMA Nanohybrids

As shown in Figure 4, the optical properties of GO were enhanced after modification. As shown in Table I, the mPEG–GO possessed a higher absorbance than the original GO–COOH at 808-nm peaks; this was because mPEG improved the stability of GO and prevented GO from aggregating in solution. After absorption with PDMAEMA, the mPEG–GO/PDMAEMA nanohybrids possessed the highest absorbance among the three kinds of materials; this may have been attributed to the positive charge of the complexes. The results may indicate that the potential of the mPEG–GO/PDMAEMA nanohybrids as a photothermal reagent is enormous.

CONCLUSIONS

A cationic gene carrier based on GO was successfully prepared by the combination of chemical modification with mPEG–NH_2

and adsorption with PDMAEMA. With the benefit of PEGylation, the mPEG–GO/PDMAEMA nanohybrids displayed acceptable cell viability. The mPEG–GO/PDMAEMA nanohybrids possessed a comparable gene-delivery efficiency to that of Lipofectamine 2000. In addition, compared to that of the original GO, the optical properties of the mPEG–GO/PDMAEMA nanohybrids were enhanced; this may indicate that mPEG–GO/PDMAEMA could be used as a photothermal reagent. In the future, the mPEG–GO/PDMAEMA nanohybrids may achieve triple therapeutic application, including gene therapy, drug delivery, and photothermal therapy.

ACKNOWLEDGMENTS

This project was supported by the National High Technology Research and Development Program of China (863; contract grant number 2012AA022501), the National Natural Science Foundation of China (contract grant numbers 81371667 and 81471727), and the Department of Education of China (contract grant number 20090001110052).

REFERENCES

1. Fire, A.; Xu, S. Q.; Montgomery, M. K.; Kostas, S. A.; Driver, S. E.; Mello, C. C. *Nature* **1998**, *391*, 806.
2. Hannon, G. *J. Nature* **2002**, *418*, 244.
3. Oh, Y. K.; Park, T. G. *Adv. Drug Delivery Rev.* **2009**, *61*, 850.
4. Resnier, P.; Montier, T.; Mathieu, V.; Benoit, J. P.; Passirani, C. *Biomaterials* **2013**, *34*, 6429.
5. Gallas, A.; Alexander, C.; Davies, M. C.; Puri, S.; Allen, S. *Chem. Soc. Rev.* **2013**, *42*, 7983.
6. Whitehead, K. A.; Langer, R.; Anderson, D. G. *Nat. Rev. Drug Discovery* **2011**, *8*, 129.
7. David, S.; Resnier, P.; Guillot, A.; Pitard, B.; Benoit, J. P.; Passirani, C. *Eur. J. Pharm. Biopharm.* **2012**, *81*, 448.
8. Sonoke, S.; Ueda, T.; Fujiwara, K.; Sato, Y.; Takagaki, K.; Hirabayashi, K.; Ohgi, T.; Yano, J. *Cancer Res.* **2008**, *68*, 8843.
9. Convertine, A. J.; Benoit, D. S. W.; Duvall, C. L.; Hoffman, A. S.; Stayton, P. S. *J. Controlled Release* **2009**, *133*, 221.
10. Sun, T. M.; Du, J. Z.; Yao, Y. D.; Mao, C. Q.; Dou, S.; Huang, S. Y.; Zhang, P. Z.; Leong, K. W.; Song, E. W.; Wang, J. *ACS Nano* **2011**, *5*, 1483.
11. Shi, S.; Shi, K.; Tan, L. W.; Qu, Y.; Shen, G. B.; Chu, B. Y.; Zhang, S.; Su, X. L.; Li, X. Y.; Wei, Y. Q. *Biomaterials* **2014**, *35*, 4536.
12. Lee, J. S.; Green, J. J.; Love, K. T.; Sunshine, J.; Langer, R.; Anderson, D. G. *Nano Lett.* **2009**, *9*, 2402.
13. Li, J.; Chen, Y. C.; Tseng, Y. C.; Mozumdar, S.; Huang, L. *J. Controlled Release* **2010**, *142*, 416.
14. Tanaka, T.; Mangala, L. S.; Vivas-Mejia, P. E.; Nieves-Alicea, R.; Mann, A. P.; Mora, E.; Han, H. D.; Shahzad, M. M. K.; Liu, X. W.; Bhavane, R. *Cancer Res.* **2010**, *70*, 3687.
15. Lin, D. S.; Cheng, Q.; Jiang, Q.; Huang, Y. Y.; Yang, Z.; Han, S. C.; Zhao, Y. N.; Guo, S. T.; Liang, Z. C.; Dong, A. *J. Nanoscale* **2013**, *5*, 4291.
16. Huang, X.; Qi, X. Y.; Boey, F.; Zhang, H. *Chem. Soc. Rev.* **2012**, *41*, 666.
17. Liu, J. Q.; Cui, L.; Losic, D. *Acta Biomater.* **2013**, *9*, 9243.
18. Yang, K.; Feng, L. Z.; Shi, X. Z.; Liu, Z. *Chem. Soc. Rev.* **2013**, *42*, 530.
19. Castro Neto, A. H.; Guinea, F.; Peres, N. M. R.; Novoselov, K. S.; Geim, A. K. *Rev. Mod. Phys.* **2009**, *81*, 109.
20. Kim, H.; Lee, D.; Kim, J.; Kim, T. I.; Kim, W. *J. ACS Nano* **2013**, *7*, 6735.
21. Sun, X. M.; Liu, Z.; Welsher, K.; Robinson, J. T.; Goodwin, A.; Zaric, S.; Dai, H. *J. Nano Res.* **2008**, *1*, 203.
22. Qin, S. Y.; Feng, J.; Rong, L.; Jia, H. Z.; Chen, S.; Liu, X. J.; Luo, G. F.; Zhuo, R. X.; Zhang, X. Z. *Small* **2014**, *10*, 599.
23. Yang, K.; Zhang, S.; Zhang, G. X.; Sun, X. M.; Lee, S. T.; Liu, Z. *Nano Lett.* **2010**, *10*, 3318.
24. Ma, X. X.; Tao, H. Q.; Yang, K.; Feng, L. Z.; Cheng, L.; Shi, X. Z.; Li, Y. G.; Guo, L.; Liu, Z. *Nano Res.* **2012**, *5*, 199.
25. Liu, Z. Z.; Lu, G. L.; Li, Y. J.; Li, Y. S.; Huang, X. Y. *RSC Adv.* **2014**, *4*, 60920.
26. Liu, Z. Z.; Li, Y. J.; Yang, Y.; Li, Y. S.; Huang, X. Y. *J. Polym. Sci. Part A: Polym. Chem.* **2013**, *51*, 4505.
27. Deng, Y.; Li, Y. J.; Dai, J.; Lang, M. D.; Huang, X. Y. *J. Polym. Sci. Part A: Polym. Chem.* **2011**, *49*, 1582.
28. Liu, Z.; Robinson, J. T.; Sun, X. M.; Dai, H. J. *J. Am. Chem. Soc.* **2008**, *130*, 10876.
29. Xu, Z. Y.; Zhu, S. J.; Wang, M. W.; Li, Y. J.; Shi, P.; Huang, X. Y. *ACS Appl. Mater. Interfaces* **2015**, *7*, 1355.
30. Xu, Z. Y.; Wang, S.; Li, Y. J.; Wang, M. W.; Shi, P.; Huang, X. Y. *ACS Appl. Mater. Interfaces* **2014**, *6*, 17268.
31. Chen, B.; Liu, M.; Zhang, L. M.; Huang, J.; Yao, J. L.; Zhang, Z. J. *J. Mater. Chem.* **2011**, *21*, 7736.
32. Kim, H.; Namgung, R.; Singha, K.; Oh, I. K.; Kim, W. *J. Bioconjugate Chem.* **2011**, *22*, 2558.
33. Kim, H.; Kim, W. *J. Small* **2014**, *10*, 117.
34. Liu, J. X.; Liu, Z.; Luo, X.; Zong, X. D.; Liu, J. Q. *Macromol. Chem. Phys.* **2013**, *214*, 2266.
35. Liu, Z.; Tabakman, S.; Sherlock, S.; Li, X. L.; Chen, Z.; Jiang, K. L.; Fan, S. S.; Dai, H. J. *Nano Res.* **2010**, *3*, 222.
36. Yang, K.; Wan, J. M.; Zhang, S.; Tian, B.; Zhang, Y. J.; Liu, Z. *Biomaterials* **2012**, *33*, 2206.
37. Liu, X. W.; Tao, H. Q.; Yang, K.; Zhang, S.; Lee, S. T.; Liu, Z. *Biomaterials* **2011**, *32*, 144.
38. Lai, J. T.; Filla, D.; Shea, R. *Macromolecules* **2002**, *35*, 6754.